Astron. Astrophys. 337, 105–112 (1998)

ASTRONOMY AND ASTROPHYSICS

Angular momentum transport in the central region of the Galaxy

Leonid M. Ozernoy[1,2], **Alexei M. Fridman**[3,4], **and Peter L. Biermann**[5]

[1] Computational Sciences Institute and Department of Physics & Astronomy, George Mason U., Fairfax, VA 22030-4444, USA (ozernoy@science.gmu.edu)
[2] Laboratory for Astronomy and Solar Physics, Goddard Space Flight Center, Greenbelt, MD 20771, USA (ozernoy@stars.gsfc.nasa.gov)
[3] Institute of Astronomy, Russian Academy of Sciences, 48 Pyatnitskaya St., 109017 Moscow, Russia (afridman@inasan.rssi.ru)
[4] Moscow State University, 18 University Prospect, 119899 Moscow, Russia
[5] Max-Planck-Institut für Radioastronomie, Auf dem Hügel 69, P.O. Box 2024, D-53010, Germany (p165bie@mpifr-bonn.mpg.de)

Received 30 April 1996 / Accepted 22 April 1998

Abstract. We discuss mechanisms for angular momentum transport in the clumpy medium of the circumnuclear disk at the Galactic center. The viscosity due to clump-clump collisions is found to be less than some critical viscosity; this meets the conditions at which a collective mode of nonaxisymmetric shear perturbations in the disk is able to grow until going into the saturation regime where fully developed turbulence is established. We find that the angular momentum transfer due to this turbulent viscosity turns out to comparable to the transport due to magnetic torques. Taken together, the turbulent and magnetic transfer of angular momentum are able to provide the inflow of mass into the central parsec with a rate of about $10^{-2}\ \mathrm{M}_{\odot}\ \mathrm{yr}^{-1}$, consistent with the available data.

Key words: Galaxy: center – accretion, accretion disks – turbulence – ISM: clouds – ISM: kinematics and dynamics

1. Introduction

Transport of angular momentum in the disks of spiral galaxies is one of the central issues in galactic dynamics. It is also of prime importance for fueling the central engines in active galactic nuclei (AGN). With regard to our own Galaxy this topic has been recently explored in a series of papers (von Linden et al. 1993a,b; Biermann et al. 1993) with the conclusion that the energy input from the SN explosions can feed the turbulence of the interstellar matter so as to provide the effective viscosity high as required to feed the star formation.

An immediate implication is that the viscous transport of angular momentum outwards is accompanied by inflow of gas inward with the rate that might be as high as $10^{-2}\ \mathrm{M}_{\odot}$/yr on the scale of hundreds pc. Earlier, a similar mass inflow rate was inferred to exist on the scale of the circumnuclear disk, i.e. at 1.5 pc $\lesssim R \lesssim 10$ pc (Genzel & Townes 1987, Jackson et al. 1993).

We also note that the star formation in the inner region of the Galaxy requires such a mass supply.

However, appropriate physical mechanism(s) which would be able to provide the necessary rate of momentum transfer within the central 10 pc or so is (are) obscure so far. The present paper aims at consideration of such mechanisms. In Sect. 2 and Appendix, we discuss viscosity in a clumpy disk due to clump interactions, both with and without self-gravity included. Sect. 3 deals with short-wave instability of the clumpy, viscous disk; the necessary condition for developing small-scale turbulence is established here. In Sect. 4, we apply this mechanism to the circum-nuclear ring at the Galactic center. The results of the paper are discussed in Sect. 5.

2. Viscosity due to cloud-cloud interactions

In a recent version of the unified model for fueling AGN, Begelman et al. (1989) proposed that the inflow of matter (driven by global axisymmetric gravitational instabilities on large scales) proceeds on small scales in the form of a 'disk' composed of randomly moving clouds, which are embedded in a low-density medium with a small filling factor. There is an essential uncertainty in our knowledge about the overall configuration, dynamics, and confinement mechanisms for thermal gas clouds observed in AGN, but as for our Galaxy, such a disk is known to exist as the circum-nuclear disk, or ring that is rather clumpy, indeed (Jackson et al. 1993). Begelman et al. (1989) assumed that the viscosity in the disk is provided by collisions between clouds. Below, this collisional mechanism of viscosity is compared with some others.

We consider the following simple model of a cloudy disk: The clouds are orbiting in an external gravitational field and have some random peculiar velocities. It is assumed that the clouds have a small filling factor and are embedded in a low-density medium that provides a confinement of the clouds. In the differentially-rotating cloudy disk, the angular momentum is transported due to cloud-cloud interactions (which include, and are not just restricted to, collisions). Let us address the shear viscosity associated with these interactions.

The most elaborated models to calculate the shear viscosity have been considered by Goldreich & Tremaine (1978) and Stewart & Kaula (1980), hereinafter referred to as GT and SK,

Send offprint requests to: L. Ozernoy

correspondingly. GT considered *contact* inelastic collisions of *non-gravitating* spherical particles obeying an anisotropic distribution function, whereas SK considered *gravitational* (elastic) encounters of particles obeying a Maxwellian distribution. In the both cases, as shown in Appendix A, the viscosity coefficient can be represented in the form

$$\nu = \frac{\sigma_v^2}{\Omega}\frac{A_i\tau}{B_i^2\tau^2+1} \ . \tag{2.1}$$

Here σ_v is the one-dimensional velocity dispersion, Ω is the orbital angular velocity in the disk, $\tau = \Omega t_i$ is the 'optical depth' to cloud-cloud interactions (see below), t_i is the free path time (index $i = c,\ G$; c stands for *c*ollisional, or *c*ontact, interactions, G stands for *g*ravitational ones), and $A_i,\ B_i$ are the constant coefficients defined below.

Collisions between the clouds result in diminishing σ_v, whereas gravitational encounters tend to increase it. For cloud-cloud collisions,

$$t_c = \left(\pi a^2 n\sigma_v\right)^{-1} , \tag{2.2}$$

where a and n are the typical size of a cloud and the spatial number density of the clouds, respectively. For gravitational encounters between the clouds

$$t_G = \frac{3\sigma_v^3}{4\sqrt{\pi}G^2m^2n} \tag{2.3}$$

(Braginskii 1965), where m is the typical mass of a cloud. Evidently, $a_G = 2\left(3\sqrt{\pi}\right)^{-1/2} Gm/\sigma_v^2$ can be considered as an effective size of the domain for gravitational influence of the cloud.

Coefficients A_i and B_i in Eq. (2.1) take the following values:

$$A_c = 0.46; \qquad B_c = 0.97$$
$$A_G = \begin{cases} 1.25 & \text{if } v = \text{const}, \\ 0.83 & \text{if } \Omega \propto r^{-3/2} \end{cases} ; \quad B_G = 1.95. \tag{2.4}$$

The optical depth τ of the disk is a convenient parameter describing how effective are the interactions between the clouds. By order of magnitude, it is nothing but the mean number of interactions suffered by a cloud in passing through the disk. More accurately,

$$\tau \simeq \pi a^2 n h \ , \tag{2.5}$$

assuming a to be the largest of geometrical and gravitational influence sizes. Here h is the thickness of the disk given by

$$h \simeq \frac{\sigma_v}{\Omega} \ . \tag{2.6}$$

Since $h \simeq \Sigma/mn$, where Σ is the surface density of the disk, Eq. (2.2) can be rewritten as

$$\tau \simeq \frac{\pi a^2}{m/\Sigma} \ , \tag{2.7}$$

which implies one more interpretation for τ: it is the covering factor, C, or the fraction of disk area covered by clouds when they are placed as a monolayer.

The filling factor of the system of clouds, i.e. the fractional volume filled by the clouds is

$$F = \frac{4}{3}\pi a^3 n \ . \tag{2.8}$$

Eqs. (2.5), (2.6), and (2.8) yield one more expression for τ containing F:

$$\tau \simeq \frac{\pi a^2 n\sigma_v}{\Omega} = \frac{3}{4}F\frac{h}{a} \ . \tag{2.9}$$

Evidently, $F \ll 1$ for any cloudy disk with $a \ll h$ unless $\tau \gtrsim h/a \gg 1$.

Here we emphasize that cloud-cloud collisisons cannot be discussed without noting that the magnetic fields permeate clouds, and are likely to make such collisions more efficient by increasing the effective cross section: When two clouds collide, it is unlikely that they just slide along a given straight flux tube. First of all, if this imagined flux tube were not exactly on a circle, then by angular momentum conservation the clouds would not go in a straight line, and second, by virtue of the general distribution of velocities it is very unlikely that two clouds would just match in proper velocities to be able to slide along a flux tube, and, third, the energy density in flux tubes is unlikely to sufficiently overpower the kinetic energy of clouds to do this. It follows that it is indeed likely that the flux tube will be twisted, thus strengthened in magnetic field, and therefore the clouds may interact even at some distance. This means that cloud-cloud collisions may involve a larger effective cross section than just the geometry would imply.

Furthermore, with magnetic loops and reconnection in the region above the disk, the effective scale height may well be larger than the scale height of the visible cloud distribution.

It follows that the estimate above may be an underestimate just as well as an overestimate; the observational fit and interpretation given to the data by von Linden et al. suggests that the viscosity derived above for cloud-cloud collisions is an underestimate.

It is instructive to compare the viscosity coefficient in a cloudy disk [Eq. (2.1)] with that in a typical thin, but continuous disk: $\nu \simeq v_s l$, where v_s and l are the sound velocity and the mean free path length, correspondingly. Qualitatively, in a continuous disk l is anticipated to be much smaller than l in a cloudy disk. If $v_s \sim \sigma_v$, the viscosity in a cloudy disk exceeds that in a continuous disk, bearing in mind some reasonable assumptions about the disk parameters. Before specifying them, we would like to discuss one more mechanism for viscosity in a cloudy disk, this time of a collective origin, proposed recently by Fridman & Ozernoy (1992).

3. Small-scale turbulent viscosity

We consider, for simplicity, both the typical size of the clouds, a, and the mean free path of the clouds, l, to obey an inequality:

$$a,\ l \ll h \ . \tag{3.1}$$

The hydrodynamics of a cloudy accretion disk with respect to 2-D nonaxisymmetric shear perturbations is similar to that for a disk with the continuous distribution of the matter explored by Fridman (1989) who found the solution of this problem in a small-amplitude, short-wave limit

$$k_r k_\varphi h^2 \gg 1, \tag{3.2}$$

where $\boldsymbol{k}$ is the wave vector. In a local rotating coordinate system, the solution for the radial component of the perturbed velocity, v_{1r}, reads:

$$\frac{v_{1r}(\tilde{t})}{v_{1r}(0)} = \frac{1+\beta^2}{1+(\beta+\tilde{t})^2} \exp(-\nu/\nu_{\rm cr}) \, , \tag{3.3}$$

where

$$\beta \equiv \frac{k_r(0)}{k_\varphi}, \;\; \tilde{t} \equiv At, \;\; A \equiv -r\frac{{\rm d}\Omega}{{\rm d}r} \, , \tag{3.4}$$

$$\nu_{\rm cr} \equiv A[k_\varphi^2 \tilde{t}(1+\beta^2+\beta\tilde{t}+\frac{1}{3}\tilde{t}^2)]^{-1} \, . \tag{3.5}$$

Here $\Omega(r)$ is the angular velocity of the disk, t is the time elapsed since the perturbations were "turned on", and $\nu_{\rm cr}$ is a (time-dependent) critical viscosity. When $\nu \ll \nu_{\rm cr}$, viscosity does not play any role in the disk dynamics.

The shortwave perturbations under consideration behave as incompressible modes. The solution (3.3) describes how the vorticity decays with time in a viscous fluid. Some limiting cases of interest can be revealed from Eqs. (3.3)–(3.5). As $t \to \infty$, there appears the asymptotic solution $\sim \exp(-\alpha t^3)$, which has been known earlier (e.g. Timofeev 1976, Zaslavskii et al. 1982). Another limiting case when viscosity is absent ($\nu = 0$), deserves a more detailed consideration.

3.1. Non-viscous case ($\nu = 0$)

In the absence of viscosity, the solution (3.3) goes into

$$v_{1r}(\tilde{t}) = \frac{v_{1r}(0)(1+\beta^2)}{1+(\beta+\tilde{t})^2} \, , \tag{3.6}$$

which was obtained by Lominadze et al. (1988). In this case, solution (3.6) implies that

$$v_{1r}(\tilde{t})k_\perp^2(\tilde{t}) = v_{1r}(0)k_\perp^2(0) = {\rm const} \, , \tag{3.7}$$

where

$$k_\perp^2(\tilde{t}) \equiv k_r^2(\tilde{t}) + k_\varphi^2, \; k_r(\tilde{t}) = k_r(0) + k_\varphi \tilde{t} \, .$$

Eq. (3.7) is a 2-D analog of the Thomson theorem on the conservation of vorticity in an incompressible fluid flow (Fridman 1989).

The solution (3.6) is shown in Fig. 1 by the solid lines. Evidently, the velocity perturbation is growing (implying instability) if the denominator in (3.6) is decreasing. At the moment when the denominator has a minimum, i.e. $\beta + \tilde{t}_* = 0$, where $\tilde{t}_*$ is given by

$$\tilde{t}_* \equiv \left| \frac{k_r(0)}{k_\varphi} \right| , \tag{3.8}$$

$v_{1r}(\tilde{t})$ reaches its maximum equal to

$$v_{1r\,\max}(\tilde{t}_*) \simeq \left(\frac{k_r(0)}{k_\varphi}\right)^2 v_{1r}(0) \tag{3.9}$$

and then goes to zero at $\tilde{t} \to \infty$. The growth of v_{1r} at $0 \le \tilde{t} \le -\beta$ is a result of a decrease of $k_\perp(\tilde{t})$ while $v_{1r}(\tilde{t})k_\perp^2(\tilde{t})$ keeps constant due to the Thomson theorem (3.7).

The minimum of the denominator in Eq. (3.6) at $(\beta+\tilde{t}_*) = 0$ implies that $(k_r(0)/k_\varphi + r\,|d\Omega/dr|\,t) = 0$ as $d\Omega/dr < 0$. Since $r > 0$, $t > 0$, the necessary condition for the perturbations to grow with time is given by

$$\frac{k_r(0)}{k_\varphi} < 0 \, . \tag{3.10}$$

Therefore, in a differentially rotating disk, the growing short-scale spiral perturbations can only be leading.

To clarify possible misunderstandings, we note several points in the following:

In Appendix B, we show that in a differentially rotating disk there are no incompressible short-wave perturbations oscillating with the epicyclic frequency at all; in a solid-body rotating disk such perturbations are stationary, in agreement with our Eqs. (3.6)-(3.10).

In Appendix C, we demonstrate that Coriolis forces are irrelevant to the solution for velocity perturbations in a plane shear layer, which we found to be similar to short-wave, low-frequency perturbations in a rotating gaseous disk. We emphasize that Coriolis forces have nothing to do with the physical meaning of our solution. The latter is associated with vorticity conservation (in the limit of small viscosity).

We consider perturbations with wavelengths *smaller* than the disk's width. Consequently our case is close to a cylinder fluid layer. Meanwhile the short-scale perturbations under the condition (3.2) are incompressible (Fridman 1989). Therefore analytical results obtained in this paper as well as in our previous papers (Fridman 1989, Fridman and Ozernoy 1992) lend to support interpretation of well-known laboratory experiments for a liquid flow between two rotating cylinders. The latter demonstrate a nonlinear instability and developed turbulence (e.g., Lukashchuk & Predtechenskii 1984). Therefore, we have all the reasons to believe that, for short-wave perturbations, a nonlinear instability is likely to occur. Likewise, in Appendix C, we show that the dynamics of short-wave incompressible perturbations in a rotating disk is completely equivalent to that in a plane shear layer. This proves the equivalence of the nonlinear instability in a plane shear layer and in the situation investigated here.

It is instructive to compare the above instability with that considered by Goldreich & Lynden-Bell (1965) (referred to as GLB hereinafter) for a self-gravitating, differentially rotating disk. There are two basic differences between our and their situations. First, different branches of growing perturbations are considered: we deal with the vortex branch while GLB do with the sound-gravitational branch. Second, the conditions for the growth of perturbations are different, too. Under condition

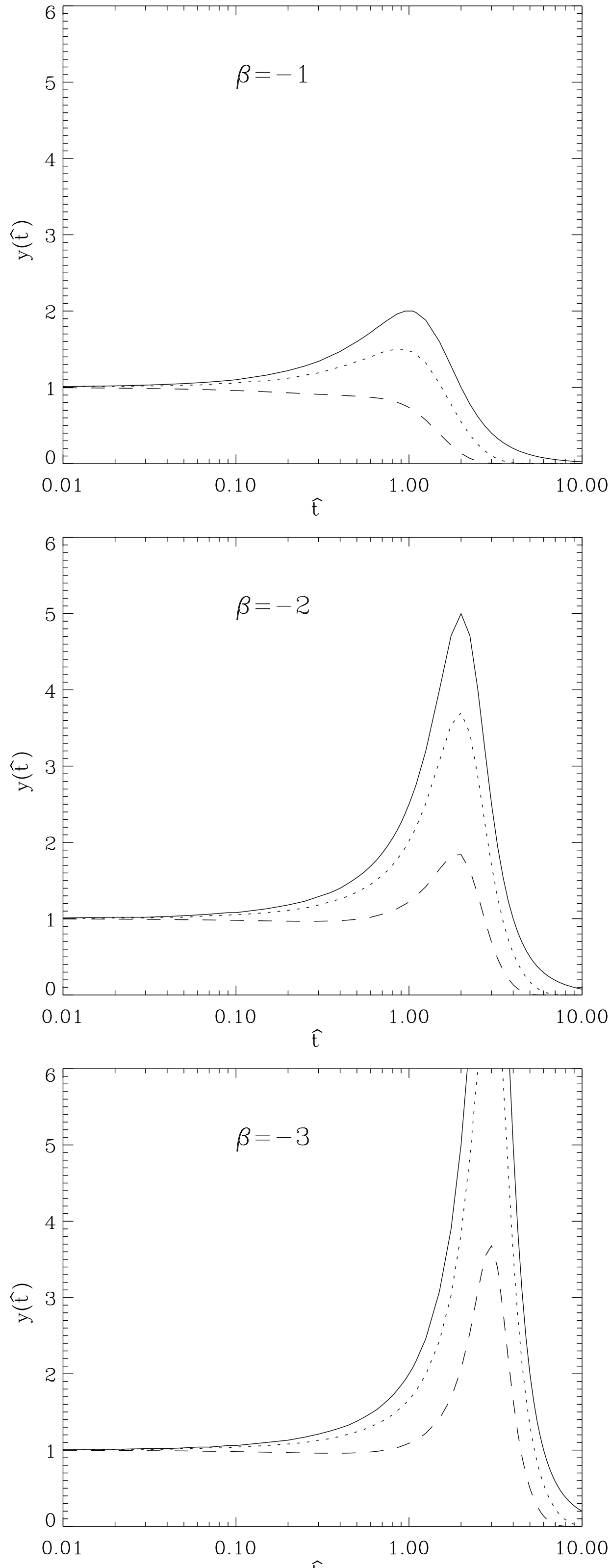

Fig. 1. "Unstable" solutions, $y \equiv v_{1r}(\tilde{t})/v_{1r}(0)$, represented by Eq. (3.3) for several values of $\beta \equiv k_r(0)/k_\varphi$. The solid lines show a non-viscous case (Eq. 3.6). A general, non-zero viscosity solution (3.3) is shown by the dotted lines for $\nu = 0.3\,\nu_{\rm crit}$ and by the dashed lines for $\nu = \nu_{\rm crit}$, where $\nu_{\rm crit}$ is defined by Eq. (3.5).

(3.10), the leading vortex perturbations grow, due to the conservation of vorticity, in an otherwise stable disk. GLB deal with the disk stable for axially-symmetrical perturbations, and the growth of their non-axially-symmetrical, long-wave perturbations proceeds due to a leading role of self-gravity. Toomre (1982) christened this growth as "swing amplification". It is worth noting that, in our case, a similar swing amplification occurs for the (vortex) short-wave perturbations and it does not require self-gravity.

3.2. General case (non-zero viscosity)

The growth of perturbations with accounting for viscosity, which is described by Eq. (3.3), is shown in Fig. 1 by the dotted and dashed lines. The "instability" described by the exact solution (3.3) is of very specific kind as v_{1r} tends to zero at $\tilde{t} \to \infty$. Nevertheless, during a finite time $\tilde{t}_*$ given by Eq. (3.8) the perturbations are in the growing regime and their amplitude increases by a factor of $k_\perp^2(0)/k_\perp^2(-\beta) = (\beta^2+1)$, which can be $\gg 1$ if $|\beta| = |k_r(0)/k_\varphi| \gg 1$.

Let us suppose that by the moment $\tilde{t} = \tilde{t}_* \equiv |\beta|$ when the amplitude of any perturbation arrives at its maximum, the viscosity does not play any essential role, i.e. $\nu \ll \nu_{\rm cr}(\tilde{t}_*)$. Though this growth in the amplitude proceeds during the time interval $\Delta\tilde{t} \simeq \tilde{t}_*$ only, it could onset the local turbulence. In this case, turbulence can be established everywhere in the disk as a superposition of the spiral perturbations originated in different points of the disk and on different moments of time; all of them have experienced a growth during $\Delta\tilde{t} \simeq \tilde{t}_*$.

The turbulence appeared as a result of the growth of the perturbations can be characterized by some turbulent viscosity, which generally is much larger than the molecular one. It is possible that a steady-state regime will emerge in which

$$\nu \to \nu_{\rm cr}(\tilde{t}_*) \equiv \nu_{\rm turb}\ . \qquad (3.11)$$

In this regime, the decay due to viscosity is strong enough to provide a steady-state level of the turbulence so that the amplitude of the perturbations is kept more or less constant in time, i.e.

$$\frac{v_{1r}(\tilde{t})}{v_{1r}(0)} \simeq 1 \ \text{ at } \ \tilde{t} \underset{\sim}{>} (\tilde{t}_*) = -\beta \simeq 1\ . \qquad (3.12)$$

Substituting Eqs. (3.11) and (3.12) into Eq. (3.3) with taking into account Eq. (3.5) and assuming that, by order of magnitude, $A \simeq \Omega$, we arrive at the following transcendental equation:

$$\exp\left(-\frac{4}{3}\,\frac{\nu_{\rm turb}\,k_\varphi^2}{\Omega}\right) \simeq \frac{1}{2}\ . \qquad (3.13)$$

Taking the logarithm of this equation one finds:

$$\nu_{\rm turb} \simeq 0.5\,\frac{\Omega}{k_\varphi^2}\ . \qquad (3.14)$$

It is straightforward to see that the basic contribution into the turbulent viscosity is given by the perturbations of the smallest k_φ's; therefore $\nu_{\rm turb} \simeq 0.5\Omega/(k_\varphi^2)_{\rm min}$. From Eqs. (3.2) and (3.12) one has $|k_\varphi| \simeq |k_r| \gg h^{-1}$, whence $|k_\varphi|_{\rm min} \simeq h^{-1}$, i.e.

$$\nu_{\rm turb} \simeq 0.5\,\Omega h^2\ . \tag{3.15}$$

By substituting $h = \sigma_v/\Omega$ into Eq. (3.15) the latter can be rewritten in the form:

$$\nu_{\rm turb} \simeq 0.5\,\frac{\sigma_v^2}{\Omega}\ . \tag{3.16}$$

It is instructive to compare the expression for the Bohm diffusion coefficient (D_B) with our Eqs. (3.14) and (3.15) for $\nu_{\rm turb}$. A well-known estimation of the Bohm diffusion coefficient for a strong turbulence plasma is given by (see e.g., Kadomtsev, 1964, or a review by Horton, 1984):

$$(D_B)_{\max} \simeq \frac{(\gamma_L)_{\max}}{(k_\perp^2)_{\min}},$$

where γ_L is the maximum linear growth rate of the drift instability, and $(k_\perp)$ is the minimum wave number, also from a linear theory. They are much the same: in our case $(\gamma_L)_{\max} \sim 0.5\,\Omega$ and instead of $k_\perp$ we substitute $(k_\varphi)_{\min} \simeq h^{-1}$. Kadomtsev obtained $(D_B)_{\max}$ by using the relationship $k_\perp\rho \sim 1$, where ρ is the Larmor radius. At $k_\perp \sim \rho^{-1}$, D_B has a maximum. But the Larmor radius in plasma corresponds to the epicyclic radius in graviphysics. The latter, in fact, is the thickness of disk, $k_\perp \simeq h^{-1}$, and this, actually, is being used here.

This viscosity whose value is given by Eq. (3.15) or (3.16) was called by Fridman & Ozernoy (1992) *anomalous* in the same sense as one introduces anomalous resistivity and anomalous diffusion in plasma physics: The origin of this viscosity is in fully developed turbulence which is established in the saturation regime described above.

Eq. (3.15) or (3.16) could be derived from dimensional arguments (of course, without the numerical coefficient) as an estimation of viscosity in a rotating disk with turbulent motions. However, we should emphasize that without an analysis such as one given above it would be impossible to reveal an underlying physical mechanism for the origin of such turbulence.

It is important to test whether the necessary condition for developing of small-scale turbulence

$$\nu < \nu_{\rm cr} \tag{3.17}$$

is met. To this end, let us find the ratio $\nu/\nu_{\rm turb}$ as a function of $\tau = \Omega t_i$, i.e. of the basic parameter that characterizes the number of interactions per one revolution:

$$\frac{\nu}{\nu_{\rm cr}} \simeq \frac{2A_i\tau}{B_i^2\tau^2+1}\ . \tag{3.18}$$

Asymptotically,

$$\frac{\nu}{\nu_{\rm cr}} \simeq \begin{cases} 2A_i\tau \ll 1 & \text{if } \tau \ll 1\ , \\ \frac{2A_i}{B_i^2}\tau^{-1} \ll 1 & \text{if } \tau \gg 1\ , \end{cases} \tag{3.19}$$

i.e. in both limits, $\tau \ll 1$ and $\tau \gg 1$, the viscosity coefficient is much less than the critical value given by Eq. (3.15) or (3.16). The function (3.18) reaches its maximum at $\tau = B_i^{-1}$, and this maximum is given by

$$\left(\frac{\nu}{\nu_{\rm cr}}\right)_{\max} \simeq \frac{A_i}{B_i}\ . \tag{3.20}$$

Even in this, the least favorable case [when $\tau \simeq 0.5$ as one can see from Eq. (2.4)] ν is less than $\nu_{\rm cr}$ by a factor of 2 or so, which is enough for small-scale turbulence to appear. Therefore the range of physical conditions under which the viscosity due to fully developed turbulence should dominate is indeed very broad.

Unlike the classical example of gravitational instability, our mechanism for the growth of shortwave perturbations has a much higher level of viscous stabilization, as it follows from the value of critical viscosity calculated above in comparison with that for a self-gravitating disk. Indeed, the growth of shortwave perturbations leads to the increase of the amplitude by a factor of

$$\frac{v_{1r}(t_*)}{v_{1r}(0)} \simeq (\frac{k_r(0)}{k_\varphi})^2 >> 1.$$

This strong inequality follows from the fact that $|k_r(0)/k_\varphi| \sim t_*/T$, where t_* is the characteristic time of the growth of perturbations and T is the period of the disk revolution. According to the perturbation theory implemented to examine instability, the condition $t_*/T >> 1$ holds (otherwise the zero-approximation of perturbation theory is not fulfilled: the equilibrium condition is broken for the time less then that of one revolution of the disk). As a result of the above inequality, a strong growth of perturbation takes place, which leads to the development of short-scale turbulence and the appearance of turbulent viscosity. A very large factor of the growth given above explains why the value of the critical turbulent viscosity, which stops the growth of perturbations, turns out to be much larger than that for the instability of a self-gravitating disk (e.g., Fridman & Polyachenko 1984, p. 41).

4. Viscosity in the circumnuclear ring

Before making numerical estimates, we list the basic parameters of the clumpy gas in the circumnuclear ring (CNR), such as the inferred clump size a, the volume filling factor F, and velocity dispersion of the clumps σ_v, taken from Jackson et al. (1993) and Güsten at al. (1987):

$$a \simeq 0.15\ {\rm pc};\quad F \sim 0.1\ -\ 0.3;\quad \sigma_v \simeq 20\ {\rm km\ s^{-1}}\ . \tag{4.1}$$

Adopting the average gas density in the clumps $n = 10^5\ {\rm cm^{-3}}$ one finds the average clump mass $m = 5\ {\rm M_\odot}$. This gives the ratio $a_G/a \simeq 10^{-3}$, which implies that elastic (gravitational) interactions between the clumps are negligible compared to inelastic ones, i.e. clump-clump collisions. In other words, gravitation plays no role in the interactions between the CNR clumps.

The mean free path of the clumps given by

$$l = \frac{4}{3}\frac{a}{F} \simeq (0.7\ -\ 2)\ \mathrm{pc}\ , \tag{4.2}$$

is rather large (even in a marginal conflict with the simplifying assumption (3.1) that $l \ll h$). The clump-clump collision rate in the CNR is given by:

$$\omega_c \simeq \frac{\sigma_v}{l} \simeq (0.3-1)\cdot 10^{-12}\mathrm{s}^{-1}, \tag{4.3}$$

i.e. $\omega_c \lesssim \Omega \simeq 2\cdot 10^{-12}\ \mathrm{s}^{-1}$ implying less than one collision per revolution. The anticipated optical depth is $\tau \simeq 0.1\ -\ 0.5$, which, according to Eq. (3.17), results in $\nu < \nu_{\rm cr}$. Therefore, the conditions for fully developed turbulence to appear, which are described at the end of Sect. 3, are met to yield the viscosity coefficient

$$\nu_{\rm turb} \simeq 1\cdot 10^{24}\ \mathrm{cm}^2\mathrm{s}^{-1}\ . \tag{4.4}$$

It is instructive to compare this result with the upper limit to viscosity derived by von Linden et al. (1993a,b). Their results were obtained by fitting an accretion disk model with arbitrary viscosity to the velocity fields of various molecular clouds, and then inferring the required kinematic viscosity from the fit. Successful fits were made in the radial range from 10 to 100 pc, with an implied kinematic viscosity of $6\,10^{26}\ \mathrm{cm}^2\ \mathrm{sec}^{-1}$ at a distance of 100 pc. Such a high viscosity is just within the limits imposed by the basic assumption of an accretion disk: The thin disk assumption implies, in the context of isotropic turbulence, that the kinematic viscosity has to be clearly less than the circular velocity times the scale height. At $r \sim 100$ pc the circular velocity is $\sim\ 200$ km/sec, and the scale height is difficult to determine; the z-distribution of clouds gives a lower limit to the scale height, and that is ~ 10 pc. This means that the kinematic viscosity has to be less than $6\,10^{26}\ \mathrm{cm}^2\ \mathrm{sec}^{-1}$; the fit by Linden et al. is obviously just at the limit. It follows either, a) that the real scale height is quite a bit larger, with a rather hard limit at roughly 1/3 of the radius, implying a hard limit of the viscosity of $2\,10^{27}\ \mathrm{cm}^2\ \mathrm{sec}^{-1}$, which should not be reached, or b) that the kinematic viscosity cannot be described with an isotropic turbulence.

The viscosity values implied by the fit to the observations of molecular clouds differ for different radii. A fit was made for clouds at 100 pc as well as 10 pc, with the viscosity decreasing for smaller radii. This radial variation may become steeper at smaller radii. The hard upper limit mentioned above would imply that it decreases as approximately $r^{1.13}$, and so would imply that the hard upper limit at 1.5 pc is $\approx 5\,10^{24}\ \mathrm{cm}^2\ \mathrm{sec}^{-1}$. We note that the result (4.4) is a factor of 5 below this upper limit. Assuming the same scaling for the kinematic viscosity derived by von Linden et al. would lead to $\approx 1.5\,10^{24}\ \mathrm{cm}^2\ \mathrm{sec}^{-1}$, which is close to Eq. (4.4); assuming the number derived from a fit at 10 pc we obtain an estimate which is near the limit.

5. Discussion

A qualitative argument presented at the end of Sect. 2 shows that the viscosity in a cloudy disk is, in general, much larger than that for a continuous disk. This assertion could be easily confirmed by numerical estimates when we address the circum-nuclear ring (CNR): in a continuous disk with similar global parameters, one would have $\nu \simeq c_s l \lesssim c_s h \simeq 10^{23}\ \mathrm{cm}^2\mathrm{s}^{-1}$, where $c_s \simeq 1$ km/s is the sound speed of the gas (Güsten et al. 1987) and $h \simeq 0.5$ pc is the thickness of the disk. What provides a much larger viscosity than it would be possible in a continuous disk is (although only partly) the clump-clump collisions. As is shown in Sect. 3, the collective mode of instability would dominate the dynamics of a clumpy disk if viscosity in the latter is less than some critical viscosity [Eq. (3.11)] whose value is given by Eq. (3.15) or (3.16). This condition is (marginally) met in the CNR, which results in the turbulent viscosity coefficient $\nu_{\rm turb}\ \simeq\ 1\ 10^{24}\ \mathrm{cm}^2\mathrm{s}^{-1}$. We note in passing that Güsten et al. (1987) suspected the existence of turbulence in the clumpy CNR, although they did not evaluate its viscosity coefficient.

It is worth mentioning that, in spite of the differences in the specific physical parameters of the clumps in the CNR and active galactic nuclei, or AGN (for the latter, see Netzer 1990), the value of $\nu_{\rm turb}$ evaluated above turns out to be in the range of the values estimated by Fridman & Ozernoy (1992) for cloudy disks in AGN. This might be relevant to the issue whether the CNR could be considered as a prototype for circum-nuclear tori around some types of AGN. (It is interesting that a large value of the viscosity in the CNR implies its rather large scale height, which is a required geometry for the AGN tori). In any case, the angular momentum transport in the CNR seems to be a template while considering similar issues both for quiescent and active galactic nuclei.

The analysis performed above has not accounted for the magnetic field in the CNR. Meanwhile several observational techniques revealed the field strength in the clouds to be ~ 1 mG (for a recent review, see Genzel et al. 1994). A magnetic field as strong as this cannot be ignored in the transport of angular momentum. Conservation of angular momentum transported by both viscous and magnetic stresses can be written for the CNR in which $v_\varphi \approx$ const in the form (Ozernoy & Genzel 1998):

$$\dot{M} = \frac{2\pi r\Sigma}{v_\varphi}\left(\xi v_A^2 + \nu_{\rm eff}\Omega\right)\left[1-\left(\frac{R_i}{r}\right)^{1/2}\right]^{-1}, \tag{5.1}$$

where $\dot{M}$ is the mass inflow rate, Σ is the surface density of the CNR, $\xi \sim 1$ is the $(-B_r/B_\varphi)$ averaged over the z-coordinate, v_A is the Alfvén velocity, $\nu_{\rm eff}$ is an effective viscosity, and $R_i \simeq 1.5$ pc is the inner radius of the ring. If we consider the CNR as a magnetized disk for which $v_A \simeq h\Omega \simeq 30$ km/s and $\nu_{\rm eff}$ is given by Eq. (4.4) the two terms in parentheses in the r.h.s. of Eq. (5.1) turn out to be comparable. This implies that while evaluating the angular momentum transport in the CNR, both magnetic and turbulent viscosity need to be accounted for. One can see that with the parameters listed above and $\Sigma \simeq 2\ 10^{-2}$ g cm^{-2} the total mass inflow rate given by Eq. (5.1) at a fiducial distance of $r = 2$ pc amounts to $\dot{M} \simeq 10^{-2}\ \mathrm{M}_\odot\ \mathrm{yr}^{-1}$.

This result is consistent with a naive, by order-of-magnitude, estimate of $\dot{M}\ \sim\ M/t_{tr}$, where M is the CNR mass and $t_{tr}\ =\ R_i^2/\nu_{\rm turb}$ is the characteristic time for the angular momentum transport: Taking $\nu_{\rm turb} \simeq 1\ 10^{24}\ {\rm cm^2 s^{-1}}$ and $M \sim 3\ 10^4\ {\rm M_\odot}$, i.e. somewhere in between 10^4 and $10^5\ {\rm M_\odot}$, the current estimates for the CNR mass (Genzel et al. 1995), one gets $t_{tr} \simeq 6\ 10^5$ yr and $\dot{M} \sim 5\ 10^{-2}\ {\rm M_\odot\, yr^{-1}}$. This is consistent as well with the inflow rate toward the Galactic center inferred from the observational data (e.g. Blitz et al. 1993, Genzel et al. 1994).

Acknowledgements. L.O. acknowledges a partial support by NASA grant NAG5-7065 and a support by the Center for Earth Observing and Space Research, GMU. A.F. is thankful to Dr. O.V. Khoruzhii for helpful discussions.

Appendix A: shear viscosity in a clumpy disk at elastic/inelastic encounters

The shear viscosity in a differentially rotating clumpy disk, with accounting for gravitational interactions between the clumps of mass m, is given by Eq. (60) in Stewart & Kaula (1980):

$$-r\Omega'\nu \;=\; A_0\sigma_v^2,$$

$$A_0 \;=\; \frac{9\sqrt{2}\,\Omega\omega_G^{-1}}{(36/5)+55\left(\Omega\omega_G^{-1}\right)^2}\,, \qquad (A1)$$

where $\Omega' \equiv {\rm d}\Omega/{\rm d}r$, and ω_G is frequency of clump-clump collisions given by

$$\omega_G = \frac{3.35\ G^2 m^2 n}{\sigma_v^3}\,. \qquad (A2)$$

Eq. (A2) corresponds to Eq. (57) of SK when one puts $\ln[1+(\sigma_v^3/Gm\Omega)^2]^{1/2} = 1$ because in a flat disk the long-range gravitational interactions could be neglected compared to the short-range ones. The value of ω_G is related to the characteristic time of gravitational encounters, t_G, given by Eq. (2.3) simply by $\omega_G^{-1} = t_G/\sqrt{2}$. By substituting Eq. (A2) into Eq. (A1), the latter could be written in the form:

$$\nu = \frac{\sigma_v^2}{\Omega}\frac{A_G\tau}{(1.95\ \tau)^2+1}\,, \qquad (A3)$$

where $A_G = 0.83$ for a Keplerian disk, $A_G = 1.25$ for a solid-body rotating disk, and $\tau = \Omega t_G$.

The viscosity coefficient for clump-clump collisions, when the clump gravity is negligible [Goldreich & Tremaine 1978, Eq. (46)], can be written in the form analogous to Eq. (A3):

$$\nu = \frac{\sigma_v^2}{\Omega}\frac{0.46\ \tau}{(0.97\ \tau)^2+1}\,. \qquad (A4)$$

Eq. (2.1) unifies the representation of viscosity both in the case when interactions are inelastic, while gravitation is negligible [Eq. (A4)] *and* in the case when gravitational encounters are dominating [Eq. (A3)].

Appendix B: character of perturbations in a differentially rotating vs. a solid-body rotating disk

Let us consider an incompressible, differentially rotating, liquid cylinder. The linearized equations of motion take the form:

$$\mathrm{div}\tilde{\boldsymbol{v}} \;=\; 0,$$

$$\frac{\partial\tilde{v}_r}{\partial t} \;+\; \Omega\frac{\partial\tilde{v}_r}{\partial\varphi} \;-\; 2\Omega\tilde{v}_\varphi \;=\; -\frac{1}{\rho}\frac{\partial\tilde{P}}{\partial r},$$

$$\frac{\partial\tilde{v}_\varphi}{\partial t} \;+\; \Omega\frac{\partial\tilde{v}_\varphi}{\partial\varphi} \;+\; \frac{\kappa^2}{2\Omega}\tilde{v}_r \;=\; -\frac{1}{\rho r}\frac{\partial\tilde{P}}{\partial\varphi}.$$

Substituting a perturbation in the form of the wave packet $f \sim \exp[-i\omega + m\varphi + \int k_r dr]$ results in the following dispersion relation ($k_\varphi \equiv m/r$):

$$\hat{\omega} \;\equiv\; \omega - m\Omega \;=\; -i(2\Omega - \kappa^2/2\Omega)\frac{k_r k_\varphi}{k^2}.$$

As always $\kappa^2 \le 4\Omega^2$, and therefore the condition of instability is $k_r k_\varphi < 0$, which corresponds to the growth of the leading spirals. Under this condition the instability is monotonous without any oscillations with epicyclic frequency. If the rotation is solid-body, one obtains $\hat{\omega} = 0$, i.e. the perturbations are stationary.

The above solution has a drawback since the r-component of the group velocity for perturbations under consideration is zero. A more detailed analysis should be performed to find out what is the role of r-dependence for Ω. This difficulty can be overcome if one considers the system in a corotating frame of reference. In this case, an exact time-dependent solution can be derived (see Fridman, 1989) which demonstrates a qualitatively the same behaviour as is obtained above. Specifically, in any differentially rotating disk whose angular velocity decreases with radius, the leading spirals grow monotonously. As for a solid-body rotating disk, all perturbations are stationary.

Note that if one would consider absolutely compressible case, i.e. $P = 0$ in the above equations, the continuity equation takes the form:

$$\frac{\partial\tilde{\rho}}{\partial t} \;+\; \rho\,\mathrm{div}\tilde{\boldsymbol{v}} \;+\; v_r\frac{d\rho}{dr} \;=\; 0,$$

and we immediately obtain

$$\hat{\omega}^2 \;=\; \kappa^2.$$

The contrast to other work is illuminating. Julian & Toomre (1966) considered perturbations in a very thin collisionless self-gravitating stellar disk. In fact, for such perturbations a collisionless *stellar* disk is absolutely compressible, in contrast to incompressible character of perturbations with wavelengths much smaller than the disk's width for a *gaseous* disk considered here. Goldreich & Lynden-Bell (1965) studied dynamics of perturbations in a gaseous disk, but only at high frequencies. Really, perturbations considered in their paper demonstrate (asymptoticaly) oscillations with sound frequency kc, where k is the wave number and c is the sound speed. As the scale of perturbations is smaller than the disk width, i.e. $kh > 1$, their frequency is higher than the epicyclic one. But as the equations of motions contain three derivatives with respect to time, they describe three modes of perturbations. Besides the two sonic high frequency modes, one mode of low frequency perturbations exists as well. What is examined in our paper is the role of *low frequency* mode in dynamics of the circumnuclear disk. As was shown in Fridman (1989), this mode does not demonstrate any oscillations and is stationary in a solid-body rotating disk.

Appendix C: Velocity perturbations in a plane shear layer

We start from linearized equations for short-wave, low-frequency perturbations in a barotropic gaseous disk in the corotating frame of reference (for derivation, see Fridman 1989):

$$k_r(t)\tilde{v}_r \;+\; k_\varphi \tilde{v}_\varphi \;=\; 0,$$
$$\frac{\partial \tilde{v}_r}{\partial t} \;-\; 2\Omega_0 \tilde{v}_\varphi \;=\; -ik_r(t)\tilde{\chi} - \nu k_\perp^2(t)\tilde{v}_r,$$
$$\frac{\partial \tilde{v}_\varphi}{\partial t} \;+\; (2\Omega_0 - A)\tilde{v}_r \;=\; -ik_\varphi \tilde{\chi} - \nu k_\perp^2(t)\tilde{v}_\varphi.$$

Here Ω_0 = const is the angular velocity of the corotating frame of reference; $A \equiv -r_0(d\Omega/dr)_0$ characterizes the value of the shear; $k_r(t) \equiv k_r + tAk_\varphi$; $k_\perp^2(t) = k_r^2(t) + k_\varphi^2$.

This system has an exact solution in the form (Fridman, 1989):

$$\tilde{v}_r(t) \;=\; \frac{k_\perp^2(0)}{k_\perp^2(t)} \tilde{v}_r(0) \exp\left[-\nu \int_0^t k_\perp^2(t)dt\right]. \qquad (C1)$$

For small t the exponential term is negligent and we come up with vorticity conservation:

$$\mathrm{curl}_z(\boldsymbol{v}) \;=\; i(k_r v_\varphi - k_\varphi v_r) \;=\; -\frac{i}{k_\varphi} k_\perp^2 v_r \;=\; \mathrm{const.} \quad (C2)$$

For a plane shear layer, a similar set of equations can be derived. The simpliest way to do this would be to put in the above system $\Omega \to 0$, $r \to \infty$, $\Omega r \to v(x)$. As a result, we obtain the following system:

$$k_x(t)\tilde{v}_x \;+\; k_y \tilde{v}_y \;=\; 0,$$
$$\frac{\partial \tilde{v}_x}{\partial t} \;=\; -ik_x(t)\tilde{\chi} - \nu k_\perp^2(t)\tilde{v}_x,$$
$$\frac{\partial \tilde{v}_y}{\partial t} \;+\; B\tilde{v}_x \;=\; -ik_y \tilde{\chi} - \nu k_\perp^2(t)\tilde{v}_y.$$

Here $B \equiv (dv/dx)_0$ characterizes the value of the shear; $k_x(t) \equiv k_x - tBk_y$; $k_\perp^2(t) = k_x^2(t) + k_y^2$. One can easily see that this system is almost similar to the previous one and it has a similar solution:

$$\tilde{v}_x(t) \;=\; \frac{k_\perp^2(0)}{k_\perp^2(t)} \tilde{v}_x(0) \exp\left[-\nu \int_0^t k_\perp^2(t)dt\right]. \qquad (C3)$$

Obviously, in a plane layer there are no any Coriolis forces at all. Nevertheless, the solution (C3) has the same form as (C1). What is relevant to the real physical meaning of our solution is conservation of vorticity (Eq. C2), which has been emphasized here.

References

Begelman, M.C., Frank, J., and Shlosman, I. 1989, in “Theory of Accretion Disks” (eds. Meyer, F., Duschl, W.J., Frank, J., & Meyer-Hofmeister, E.). Kluwer, Dordrecht, p.373

Biermann, P.L., Duschl, W.J., & von Linden, S. 1993, A&A, 275, 153

Blitz, L., Binney, J., Lo, K.Y., Bally, J., & Ho, P.T.P. 1993, Nature 361, 417

Braginskii, S.I. 1965, in “Reviews of Plasma Physics” (ed. Leontovich, M.A.). Consultants Bureau, N.Y., v.1, p. 205

Fridman, A.M. 1989, Sov. Astron. Lett. 15, 487

Fridman, A.M., & Polyachenko, V.L. 1984 “Physics of Gravitating Systems”, v.2, Ch. 7, Springer-Verlag, and papers by R. Miller, F. Hohl, and others cited in that book

Fridman, A. & Ozernoy, L. 1992, in “Testing the AGN Paradigm” (eds. Holt, S.S., Bennett, C.L., & Trimble, V.) AIP Conf. Proc. 222, 280

Genzel, R., Hollenbach, D., & Townes, C.H. 1994, Rep. Progr. Phys. 57, 417

Genzel, R. & Townes, C.H. 1987, Ann. Rev. Astr. Ap. 25, 377

Goldreich, P. & Lynden-Bell, D. 1965, MNRAS, 130, 125

Goldreich, P. & Tremaine, S. 1978, Icarus 34, 227 (GT)

Güsten, R., Genzel, R., Wright, M.C.H., Jaffe, D.T., Stutzki, J., & Harris, A.I. 1987, ApJ, 318, 124

Horton “Drift wave turbulence and anormalous transport”, Handbook of Plasma Physics, v.2, p.383, North-Holland Phys. Publ., 1984

Julian, W.H. & Toomre, A. 1966, ApJ 146, 810

Kadomtsev, B., Sov. Phys. JETP, 1964, v.18, p.847

Jackson, J.M., Geiss, N., Genzel, R., Harris, A.I., Madden, S., Poglitsch, A., Stacey, G.J., & Townes, C.H. 1993, ApJ, 402, 173

Lominadze, D.G., Chagelishvili, G.D., & Chanishvili, R.G. 1988, Sov. Astron. Lett. 14, 364

Lukashchuk, S.N. & Predtechenskii, A.A. 1984, DAN SSSR, 274, 1317

Netzer, H. 1990, in “Active Galactic Nuclei” (eds. Courvoisier, T.J.-L., and Mayor, M.). Springer, Berlin, p. 57

Ozernoy, L.M. & Genzel, R. 1998 (to be submitted)

Stewart, G.L. & Kaula, W. 1980, Icarus 44, 154 (SK)

Timofeev, A.V. 1976, Sov. J. Plasma Physics, 2, 280

Toomre, A. 1981, In “Structure and Evolution of Normal Galaxies. Ed. S.M.Fall and D.Lynden-Bell. Cambridge University Press, p. 111

von Linden, S., Duschl, W.J., & Biermann, P.L. 1993a, A&A, 269, 169

von Linden, S., Biermann, P.L., Duschl, W.J., Lesch, H. & Schmutzler, T. 1993b, A&A, 280, 468

Zaslavskii, G.M., Meitlis, V.P., & Filonenko, N.N. 1982, “Wave Interactions in Nonuniform Media” (in Russian). Nauka, Novosibirsk